Physics and Imaging in Radiation Oncology 27 (2023) 100458

Contents lists available at ScienceDirect

Physics and Imaging in Radiation Oncology

journal homepage: www.sciencedirect.com/journal/physics-and-imaging-in-radiation-oncology

Original Research Article

Optimal time for early therapeutic response prediction in nasopharyngeal carcinoma with functional magnetic resonance imaging

Alan W.L. Mui [a,b,*], Anne W.M. Lee [b], Wai-Tong Ng [b], Victor H.F. Lee [b], Varut Vardhanabhuti [c], Shei-Yee Man [a], Daniel T.T. Chua [d], Xin-Yuan Guan [b]

[a] Department of Radiotherapy, Hong Kong Sanatorium and Hospital, Hong Kong, China
[b] Department of Clinical Oncology, Li Ka Shing Faculty of Medicine, The University of Hong Kong, Hong Kong, China
[c] Department of Diagnostic Radiology, Li Ka Shing Faculty of Medicine, The University of Hong Kong, Hong Kong, China
[d] Department of Medicine, Hong Kong Sanatorium and Hospital, Hong Kong, China

ARTICLE INFO

Keywords:
DCE-MRI
DW-MRI
MRS
ADC
Nasopharyngeal Carcinoma

ABSTRACT

Background and Purpose: Physiological changes in tumour occur much earlier than morphological changes. They can potentially be used as biomarkers for therapeutic response prediction. This study aimed to investigate the optimal time for early therapeutic response prediction with multi-parametric magnetic resonance imaging (MRI) in patients with nasopharyngeal carcinoma (NPC) receiving concurrent chemo-radiotherapy (CCRT).

Material and Methods: Twenty-seven NPC patients were divided into the responder (N = 23) and the poor-responder (N = 4) groups by their primary tumour post-treatment shrinkages. Single-voxel proton MR spectroscopy (^{1}H-MRS), diffusion-weighted (DW) and dynamic contrast-enhanced (DCE) MRI were scanned at baseline, weekly during CCRT and post-CCRT. The median choline peak in ^{1}H-MRS, the median apparent diffusion coefficient (ADC) in DW-MRI, the median influx rate constant (K^{trans}), reflux rate constant (K_{ep}), volume of extravascular-extracellular space per unit volume (V_e), and initial area under the time-intensity curve for the first 60 s (iAUC60) in DCE-MRI were compared between the two groups with the Mann-Whitney tests for any significant difference at different time points.

Results: In DW-MRI, the percentage increase in ADC from baseline to week-1 for the responders (median = 11.39%, IQR = 18.13%) was higher than the poor-responders (median = 4.91%, IQR = 7.86%) (p = 0.027). In DCE-MRI, the iAUC60 on week-2 was found significantly higher in the poor-responders (median = 0.398, IQR = 0.051) than the responders (median = 0.192, IQR = 0.111) (p = 0.012). No significant difference was found in median choline peaks in ^{1}H-MRS at all time points.

Conclusion: Early perfusion and diffusion changes occurred in primary tumours of NPC patients treated with CCRT. The DW-MRI on week-1 and the DCE-MRI on week-2 were the optimal time points for early therapeutic response prediction.

1. Introduction

Nasopharyngeal carcinoma (NPC) is an endemic malignancy in Southern China and Southeast Asia. It is not easy to be detected during the early stage of malignant development. Over 70% of NPC patients are diagnosed with advanced stage III or IV diseases [1]. Concurrent chemo-radiotherapy (CCRT) is the standard treatment for stage II or above [2], which makes up over 85% of NPC patients [1]. The CCRT lasts for about seven weeks. Therapeutic response to CCRT is usually assessed by surveillance examinations at around 12 weeks post-CCRT when the treatment side effects subsided and enough time allowed for tumour regression [3,4]. Additional radiation boosts have been recommended for patients with persistent local disease [5].

Tumour physiological changes happen much earlier than morphological [6]. Recent studies showed that functional magnetic resonance imaging (fMRI) could be used to examine early therapeutic response predictions in nasopharyngeal tumours [7,8]. Physiological changes in tumours, including alternations in metabolite concentrations, diffusivity and vascular permeability, can be potential biological indicators for early therapeutic response prediction in NPC. Techniques such as proton

* Corresponding author at: Department of Radiotherapy, Hong Kong Sanatorium and Hospital, 2 Village Road, Happy Valley, Hong Kong, China.
E-mail address: alan.wl.mui@hksh.com (A.W.L. Mui).

https://doi.org/10.1016/j.phro.2023.100458
Received 16 February 2023; Received in revised form 26 May 2023; Accepted 12 June 2023
Available online 21 June 2023

Table 1
Patient and tumour characteristics.

Patient Characteristics		No. of Patient	%
Age (years)			
	Range 26-66		
	Median 49		
Sex			
	Male	22	81.5
	Female	5	18.5
T-category			
	T1	9	33.4
	T2	4	14.8
	T3	10	37.0
	T4	4	14.8
Stage			
	II	6	22.2
	III	14	51.9
	IV	7	25.9

magnetic resonance spectroscopy (^{1}H-MRS), diffusion-weighted (DW-) and dynamic contrast-enhanced (DCE-) MRI have been recommended for monitoring physiological changes in head and neck cancers [9–11].

This study aimed to investigate the early tumour physiological changes in NPC patients receiving CCRT with regular ^{1}H-MRS, DW-MRI and DCE-MRI, so that the optimal time to predict the therapeutic responses with these fMRI techniques can be identified.

2. Material and Methods

This prospective study was approved by the hospital research ethics committee (REC-2017–06) in compliance with the ethical standards for human research in the Declaration of Helsinki and the Good Clinical Practice (GCP). Informed consents were obtained from the patients.

Twenty-seven patients pathologically diagnosed with NPC were included. Patient characteristics are summarised in Table 1. They were classified by the 8th edition of the American Joint Committee on Cancer (AJCC) TNM classification system [12] with stage II or above NPC who were eligible for CCRT. Cisplatin-based chemotherapy at a dosage of 40 mg/m^2 was given in 7 weekly cycles. RT was delivered with helical tomotherapy by Radixact (Accuray Inc., Sunnyvale, CA, USA) with 70–75 Gy in 33–35 fractions over 6.6–7 weeks to the gross nasopharyngeal tumours. Patients were scanned with fMRI before the CCRT, weekly during the CCRT and median 10 days after completion of CCRT. The ^{1}H-MRS and DW-MRI were acquired at all these time points, whereas the DCE-MRI was obtained at pre-treatment, week 1 to week 3, and post-treatment time points only in view of the potential gadolinium contrast agent toxicity.

2.1. Imaging

All patients were immobilised in thermoplastic casts and were scanned in a 1.5 T MAGNETOM Aera MR-Simulator (Siemens Healthcare, Erlangen, Germany) dedicated to RT planning. The scans were done on a flat couch embedded with a posterior 32-channel spine coil array and a pair of 4-channel large flex receiver coils with interfaces which were wrapped around the head region with a pair of bilateral coil holders (Orfit Industry, Wijnegem, Belgium). The primary nasopharyngeal tumour was localised by the morphological images acquired with a sagittal 3D T2-weighted turbo spin echo (TSE) SPACE sequence.

The ^{1}H-MRS scans were performed using a single voxel approach. It was centred at the spot where the highest standardised uptake value (SUV) was identified in the pre-treatment diagnostic positron emission tomography (PET) scan. The ^{1}H-MRS were acquired by water-suppressed point-resolved spectroscopy (PRESS) sequence with TR/TE of 1470/30 ms, NEX 256, volume of interest (VOI) in size of 15 × 15 × 15 mm^3 and acquisition time of 6 min 24 sec.

The DW-MRI scans were acquired in an interleaved fashion using an axial 2D diffusion-weighted multi-shot readout-segment echo-planar imaging (RS-EPI) RESOLVE sequence with GRAPPA acceleration technique. The DW-MRI protocol was as follows: FOV = 220 × 220 mm^2, matrix size = 112 × 112, slice thickness = 3.5 mm with 10% gap, voxel size = 2 × 2 × 3.5 mm^3, slice number = 20, TR/TE1/TE2 = 3890/51/78 ms, b-values = 50(2), 800(4) sec/mm^2. The scan volume was set as contiguous axial sections through the primary nasopharyngeal lesion with an acquisition time of 6 min 27 sec.

The DCE-MRI scans were performed in an axial 3D T1-weighted TWIST VIBE sequence with protocol as follows: FOV = 260 × 260 mm^2, matrix size = 192 × 154, slice thickness = 3.5 mm, voxel size = 1.4 × 1.4 × 3.5 mm^3, slice number = 30, TR/TE = 6.28/2.38 ms, flip angle = 9°. The scan was repeated for 60 dynamic phases with a temporal resolution of 4.7 sec. The images were acquired with two initial dynamic phases without contrast. A dosage of 0.1 mmol/kg of gadobutrol (Gadovist, Bayer Vital GmbH, Leverkusen, Germany) contrast agent was injected at the third dynamic phase using a power injector at a constant flow rate of 2.5 mL/sec, followed by a 20 mL normal saline flushed at the same flow rate. The concentration of the contrast agent was calculated from the MR signal using preceding baseline mapping scans with two flip angles (2° and 15°, TR/TE = 3.8/1.34 ms). These flip angles were chosen as this combination achieved the smallest overestimation for K^{trans} in primary tumours of head and neck cancers [13]. The DCE-MRI acquisition time was 4 min 42 sec.

2.2. Post-processing

The ^{1}H-MRS, DW-MRI and DCE-MRI images were all post-processed by the image reading application syngo.via (Siemens Healthcare, Erlangen, Germany) provided by the MR-Simulator vendor. The choline intensity peaks in ^{1}H-MRS and the apparent diffusion coefficient (ADC) in DW-MRI were measured. Tofts compartment model was employed in the DCE-MRI measurements [14]. Each voxel of tissue was differentiated into parenchymal cells, blood vessels and extracellular extravascular space (EES). Perfusion parameters, including the influx rate from blood vessels into EES (K^{trans}), the reflux rate from EES back into plasma (K_{ep}), the volume of EES per unit volume of tissue (V_e) and the initial area-under-curve for the first 60 sec (iAUC60) of contrast arrival from the time-intensity curve (TIC), were measured. The arterial input function (AIF) was modelled by population-based technique [15], with the subject AIF curve best fitted to either fast [16], intermediate [17] or slow [18] documented population average suggested by the vendor application. The VOI for ADC and perfusion parameter measurements were initially localised to the nasopharyngeal tumour by reviewing the patient's most updated diagnostic MR and/or PET scans. Both ADC and perfusion shared the same VOI for volumetric three-dimensional measurements. The VOIs for subsequent measurements were traced with anatomical reviews in the multiple morphological images acquired weekly. They were delineated by the same dosimetrist and checked by the same oncologist with 23 and 33 years of experiences in radiation oncology respectively.

Patients were divided into the responder and poor-responder groups according to their primary tumour post-treatment shrinkages in morphological MR images with more or less than 50% volume respectively [19]. The differences in median choline peak, ADC, K^{trans}, K_{ep}, V_e and iAUC60 at all time points, as well as their percentage changes from baseline at all time points were analysed between the two groups by Mann-Whitney tests for any statistical significance.

3. Results

Patients were classified as the responders (N = 23) and the poor-responders (N = 4) with their mean post-treatment tumour volumes shrank to 31.6% (standard deviation, SD = 7.8%) and 86.3% (SD = 11.3%) of their pre-treatment volumes respectively.

In ^{1}H-MRS, there were 65.8% of the MR spectra with fitting error less

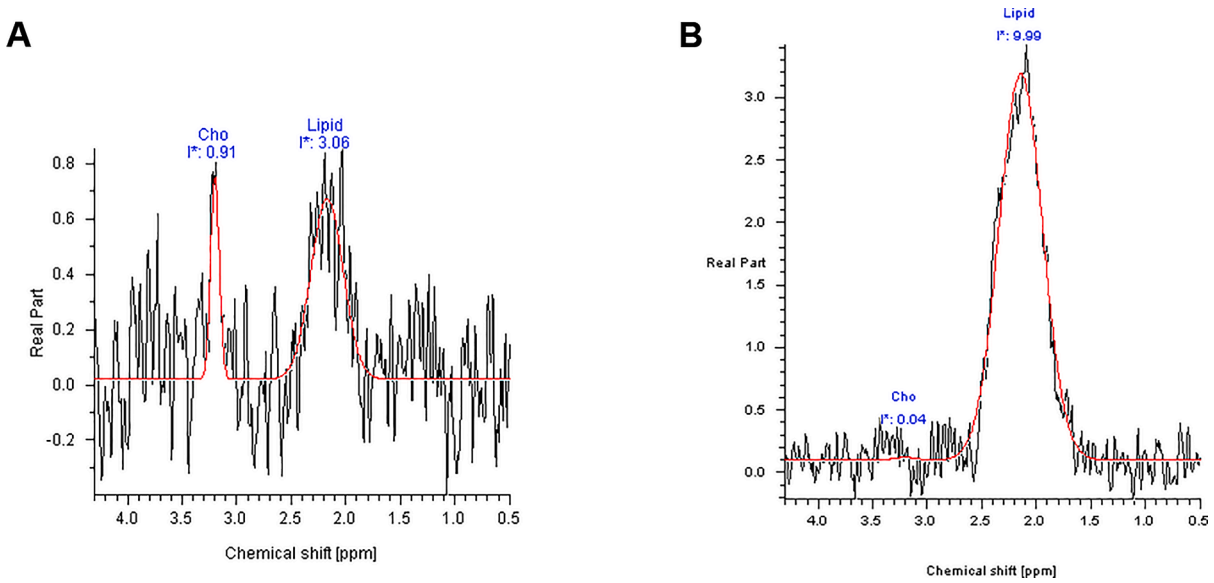

Fig. 1. Examples of interpretable MR spectrum **(A)** and non-interpretable MR spectrum **(B)** for nasopharyngeal tumours.

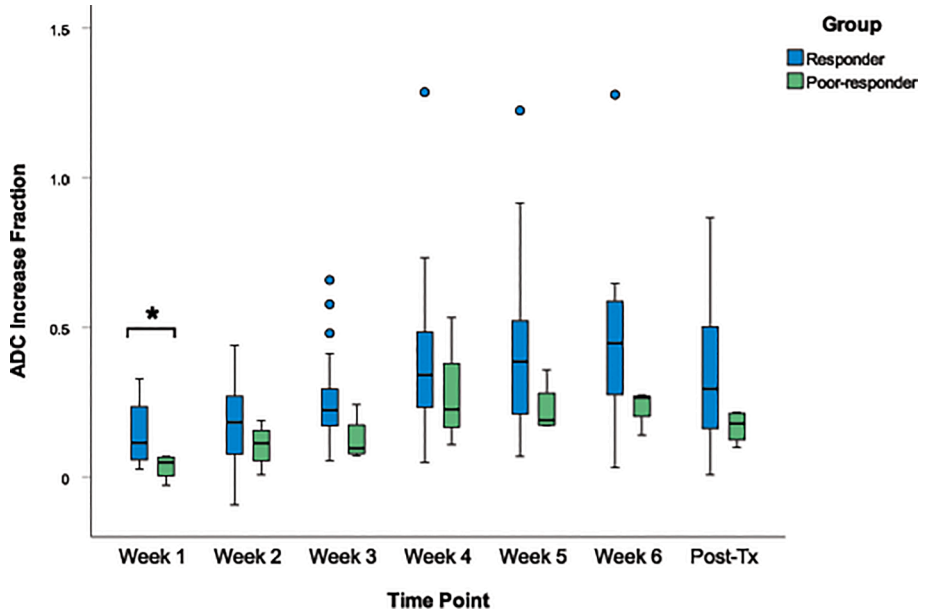

Fig. 2. The median percentage increases in ADC values at different time points. The bottom and top edges of boxes represent the 1st and the 3rd quartiles of values respectively. The circle symbols indicate the outliers. The asterisk (*) flags the statistical significance level with p-value <0.05.

than 3% which were regarded as interpretable spectra. Choline peak was the only identifiable peak in the MR spectra. No significant difference could be found between the two groups. Examples of interpretable and non-interpretable spectra are shown in Fig. 1.

In DW-MRI, overall gradual increases in ADC values were observed in both groups of patients. The percentage increases of ADC from baseline at all time points were compared. The median percentage increase in ADC value after the first week of CCRT (ΔADC_{Week1}) for the responder group was 11.39% (interquartile range, IQR = 18.13%), which was higher than that of the poor-responder group 4.90% (IQR = 7.86%) (p = 0.027). The median percentage increases in ADC values at different time points are shown in Fig. 2.

In DCE-MRI, the median iAUC60 on week 2 for the poor-responder group was 0.398 (range = 0.051), which was higher than that of the responder group at 0.192 (IQR = 0.111) (p = 0.012). The median iAUC60s at different time points are shown in Fig. 3. Examples of iAUC60 parametric maps for a responder and a poor-responder are shown in Fig. 4. Significant differences were not found in K^{trans}, K_{ep} and V_e.

4. Discussion

This study showed that early perfusion and diffusion changes occurred in the nasopharyngeal tumours treated with CCRT. The median percentage increase in ADC value after the first week and the median iAUC60 at week 2 were significantly different in responders and poor-responders. They might be used as biological indicators to predict therapeutic responses of NPC patients receiving CCRT.

To the best of our knowledge, no other studies have monitored the nasopharyngeal tumour with weekly multi-parametric MRI and reported its early physiological changes receiving CCRT. We identified the changes in nasopharyngeal tumour diffusability were most significantly

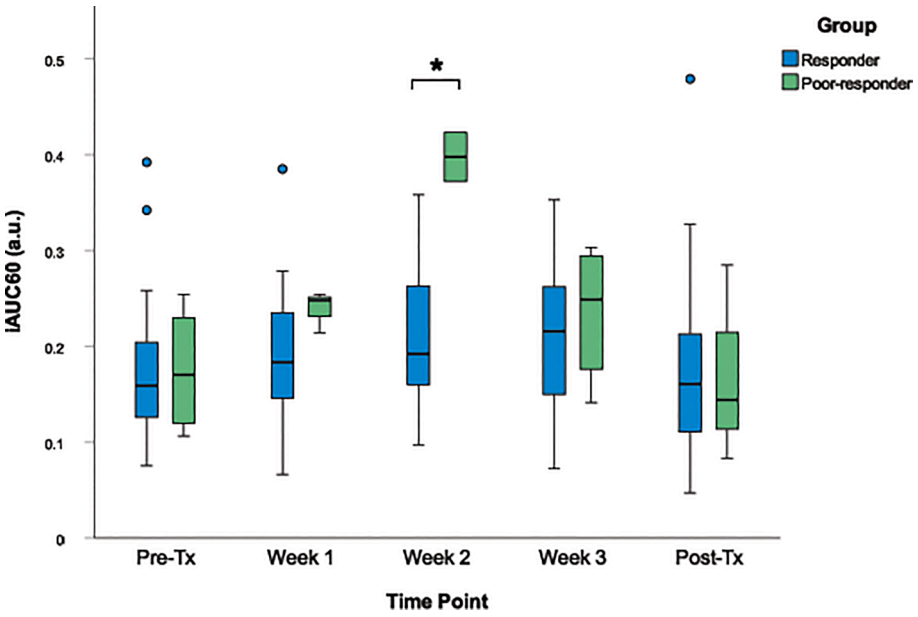

Fig. 3. The median iAUC60 at different time points. The bottom and top edges of boxes represent the 1st and the 3rd quartiles of values respectively. The circle symbols indicate the outliers. The asterisk (*) flags the statistical significance level with p-value <0.05.

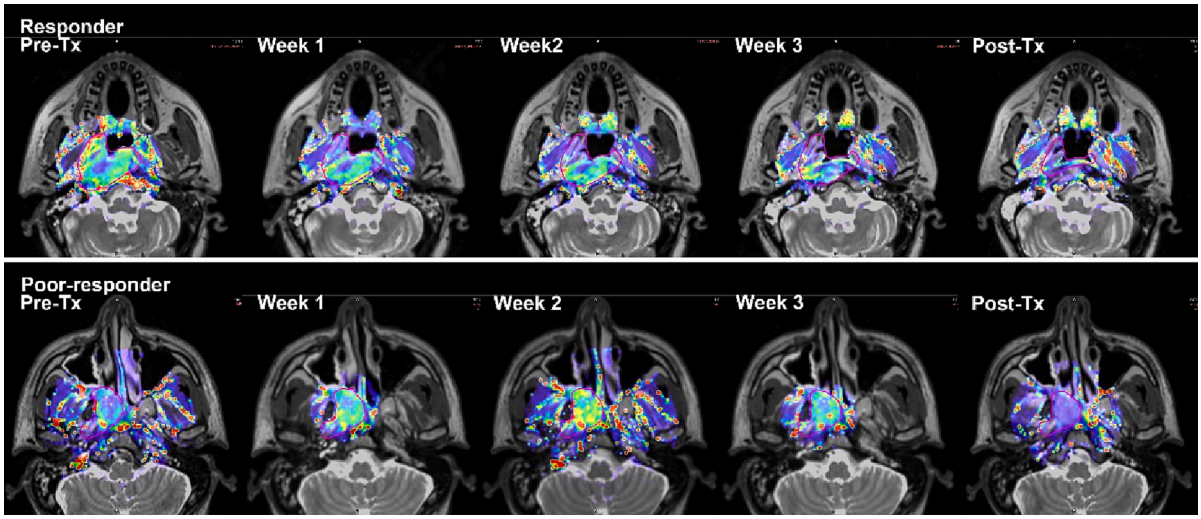

Fig. 4. Examples of the iAUC60 changes for a responder **(upper row)** and a poor-responder **(lower row)**. The gross tumours were delineated in magenta contour. Conspicuous increase in iAUC60 was observed in the poor-responder on week 2 DCE-MRI scan. (For interpretation of the references to colour in this figure legend, the reader is referred to the web version of this article.)

different between the responders and poor-responders after receiving the first week of CCRT. Also, the tumour vascular permeability significantly differed between the two groups after two weeks of CCRT.

DW-MRI is one of the most widely used MR techniques to assess tumour cellularity in clinical practice [20,21]. Water molecules move around randomly in tissue with Brownian motions. The movement of water molecules causes loss of MR signal through magnetic spin dephasing [22]. The presence of chaotic cancerous structures and increased tissue cellularity cause different degrees of impedance to water molecule motions, resulting in different degrees of MR signal loss. This signal loss over time is quantitatively derived as the ADC value. Therefore, the ADC value indirectly reflects the cellularity of tissue [23]. We showed that in NPC patients with good responses to CCRT, their ADC value percentage increases from pre-treatment to week 1 were significantly higher than the poor-responders. This indicated that the rapid reduction in tumour cellularity was an early physiological event in a responsive nasopharyngeal tumour, even at a low dosage of just one week of CCRT. And this relatively low dosage was sufficient to differentiate the ultimate responses to CCRT.

DCE-MRI assesses tumour vascularity by quantitative measurement of contrast agent influx and reflux between the intravascular and extravascular-extracellular compartments by time trace of contrast concentration [24]. The proliferation of tumour cells requires angiogenesis and increased vascular leakiness to support, particular in those hypoxic tumours [25]. Lu, et al. [26] reported that NPC patients with poor prognoses were associated with hypoxia-inducible factor 1-alpha (HIF-1α) and vascular endothelial growth factor (VEGF) expression. Their findings were supported by another study by Hui, et al. [25] which showed similar HIF-1α and VEGF co-expression with other proangiogenic factors in NPC patients with poor prognosis. Our study showed that NPC patients with poor responses to CCRT had significant higher iAUC60 on the second week of DCE-MRI than those with good responses.

The iAUC60 reflects the influx and early reflux of contrast agent between the compartments. Tumours with leakier vasculatures are characterized by higher iAUC60. Our results were in line with the phenomenon that nasopharyngeal tumours with poor responses to CCRT are highly vascularized. Their vasculatures were leakier than others as endothelial tip cell migration and degradation were elevated in the process of angiogenesis [27]. It might be explained by the fact that the cumulative dosage of two weeks of CCRT has promoted the degradation and further breakdown of the originally less articulated endothelial cell lining.

Our results identified that tumour physiological changes in cellularity and vascular permeability that occurred within two weeks of CCRT commencement were significantly different in responders and poor-responders. These changes happened at a relatively early phase of the seven-week treatment course. This early prediction of therapeutic responses is desirable. Patients with poor responses to CCRT will not be left unaware until the surveillance is done months after treatment completion. Clinicians might have an early alert to the poor-responders and thus better cancer treatment management for their patients. They might consider if adaptive RT plans with integrated boost can be adopted in the later phase of the CCRT course. It might even be possible to utilize the DW-MRI or DCE-MRI parametric maps for personalized biological target volume delineation to improve tumour control. However, when applying these functional parameters quantitatively for therapeutic response monitoring and treatment personalization, cautions must be taken to ensure the scanner repeatability so that any changes in functional parameters are truly reflecting therapeutic responses on patients but not drifts in scanner performance [28].

Our fMRI study has several limitations. First, the sample size was relatively small, and the group sizes were imbalanced. They could be improved with more recruitment of subjects. Second, limited by the patient logistics of the hospital, patients seldom came back for their long-term clinical follow-up. The post-treatment assessment was constrained to a relatively early endpoint. The availability of long-term follow-up data, for instance, loco-regional relapse and distant metastasis data, would give better robustness and significance to this study. Third, the VOI averages were used in measuring the fMRI parameters without considering the heterogeneity within the VOI. It could be addressed by having a histogram approach in parameter analysis [23,29]. Lastly, the interpretable rate of ^{1}H-MRS was rather unsatisfactory. It was probably caused by the hardware limitations of the MR-Simulator, which was not comparable to the diagnostic-graded MR scanner. A stronger magnetic field or better coil design might improve the ^{1}H-MRS sensitivity and the interpretable spectrum rate.

In conclusion, early perfusion and diffusion changes occurred in the primary tumours of NPC patients treated with CCRT. The DW-MRI on week 1 and the DCE-MRI on week 2 were the optimal time points for early therapeutic response prediction in NPC patients receiving CCRT. Further studies with larger cohort would be needed to validate the robustness of the proposed time points.

Declaration of Competing Interest

The authors declare that they have no known competing financial interests or personal relationships that could have appeared to influence the work reported in this paper.

Acknowledgement:

Nil.

Grant Support.

Nil

References

[1] Hospital Authority. Hong Kong Cancer Registry, http://www3.ha.org.hk/cancereg/; 2019.

[2] Lee A. Current Management Strategies for Non-Metastatic Nasopharyngeal Cancer. Am J Cancer 2006;5:383–92. https://doi.org/10.2165/00024669-200605060-00005.

[3] Lv JW, Zhou GQ, Li JX, Tang LL, Mao YP, Lin AH, et al. Magnetic Resonance Imaging-Detected Tumor Residue after Intensity-Modulated Radiation Therapy and its Association with Post-Radiation Plasma Epstein-Barr Virus Deoxyribonucleic Acid in Nasopharyngeal Carcinoma. J Cancer 2017;8:861–9. https://doi.org/10.7150/jca.17957.

[4] Kwong DLW, Nicholls J, Wei WI, Chua DTT, Sham JST, Yuen PW, et al. The time course of histologic remission after treatment of patients with nasopharyngeal carcinoma. Cancer 1999;85:1446–53. https://doi.org/10.1002/(SICI)1097-0142(19990401)85:7<1446::AID-CNCR4>3.0.CO;2-3.

[5] Teo P, Leung S, Choi P, Lee W, Johnson P. Afterloading radiotherapy for local persistence of nasopharyngeal carcinoma. Br J Radiol 1994;67:181–5.

[6] Kumagai Y, Toi M, Inoue H. Dynamism of tumour vasculature in the early phase of cancer progression: outcomes from oesophageal cancer research. Lancet Oncol 2002;3:604–10. https://doi.org/10.1016/S1470-2045(02)00874-4.

[7] Chen Y, Liu X, Zheng D, Xu L, Hong L, Xu Y, et al. Diffusion-weighted magnetic resonance imaging for early response assessment of chemoradiotherapy in patients with nasopharyngeal carcinoma. Magn Reson Imaging 2014;32:630–7. https://doi.org/10.1016/j.mri.2014.02.009.

[8] Zheng D, Chen Y, Liu X, Chen Y, Xu L, Ren W, et al. Early response to chemoradiotherapy for nasopharyngeal carcinoma treatment: Value of dynamic contrast-enhanced 3.0 T MRI. J Magn Reson Imaging 2015;41:1528–40. https://doi.org/10.1002/jmri.24723.

[9] Bezabeh T, Odlum O, Nason R, Kerr P, Sutherland D, Patel R, et al. Prediction of Treatment Response in Head and Neck Cancer by Magnetic Resonance Spectroscopy. Am J Neuroradiol 2005;26:2108–13.

[10] Chikui T, Kitamoto E, Kawano S, Sugiura T, Obara M, Simonetti AW, et al. Pharmacokinetic analysis based on dynamic contrast-enhanced MRI for evaluating tumor response to preoperative therapy for oral cancer. J Magn Reson Imaging 2012;36:589–97. https://doi.org/10.1002/jmri.23704.

[11] Yu XP, Hou J, Li FP, Hu Y, Lu Q, Wang L, et al. Intravoxel incoherent motion MRI for predicting early response to induction chemotherapy and chemoradiotherapy in patients with nasopharyngeal carcinoma. J Magn Reson Imaging 2016;43:1179–90. https://doi.org/10.1002/jmri.25075.

[12] Brierley J, Gospodarowicz MK, Wittekind C. TNM classification of malignant tumours. Eighth edition. ed. Chichester, West Sussex, UK, Hoboken, NJ: John Wiley & Sons, Inc.; 2017.

[13] Yuan J, Chow SKK, Yeung DKW, Ahuja AT, King AD. Quantitative evaluation of dual-flip-angle T1 mapping on DCE-MRI kinetic parameter estimation in head and neck. Quant Imaging Med Surg 2012;2:245–53. https://doi.org/10.3978/j.issn.2223-4292.2012.11.04.

[14] Tofts PS. Modeling tracer kinetics in dynamic Gd-DTPA MR imaging. J Magn Reson Imaging 1997;7:91–101. https://doi.org/10.1002/jmri.1880070113.

[15] Rata M, Collins DJ, Darcy J, Messiou C, Tunariu N, Desouza N, et al. Assessment of repeatability and treatment response in early phase clinical trials using DCE-MRI: comparison of parametric analysis using MR- and CT-derived arterial input functions. Eur Radiol 2016;26:1991–8. https://doi.org/10.1007/s00330-015-4012-9.

[16] Orton MR, d'Arcy JA, Walker-Samuel S, Hawkes DJ, Atkinson D, Collins DJ, et al. Computationally efficient vascular input function models for quantitative kinetic modelling using DCE-MRI. Phys Med Biol 2008;53:1225–39. https://doi.org/10.1088/0031-9155/53/5/005.

[17] Parker GJM, Roberts C, Macdonald A, Buonaccorsi GA, Cheung S, Buckley DL, et al. Experimentally-derived functional form for a population-averaged high-temporal-resolution arterial input function for dynamic contrast-enhanced MRI. Magn Reson Med 2006;56:993–1000. https://doi.org/10.1002/mrm.21066.

[18] Weinmann HJ, Laniado M, MÜTzel W.. Pharmacokinetics of GdDTPA/dimeglumine after intravenous injection into healthy volunteers. Physiol Chem Phys Med NMR 1984;16:167–72.

[19] Yang S-N-M-D, Liao C-Y-M-D, Chen S-W-M-D, Liang J-A-M-D, Tsai M-H-M-D, Hua C-H-M-D, et al. Clinical Implications of the Tumor Volume Reduction Rate in Head-and-Neck Cancer During Definitive Intensity-Modulated Radiotherapy for Organ Preservation. Int J Radiat Oncol Biol Phys 2011;79:1096–103. https://doi.org/10.1016/j.ijrobp.2009.12.055.

[20] Fliedner FP, Engel TB, El-Ali HH, Hansen AE, Kjaer A. Diffusion weighted magnetic resonance imaging (DW-MRI) as a non-invasive, tissue cellularity marker to monitor cancer treatment response. BMC Cancer 2020;20:134. https://doi.org/10.1186/s12885-020-6617-x.

[21] Surov A, Meyer HJ, Wienke A. Correlation between apparent diffusion coefficient (ADC) and cellularity is different in several tumors: a meta-analysis. Oncotarget 2017;8:59492–9. https://doi.org/10.18632/oncotarget.17752.

[22] Descoteaux M, Poupon C. Diffusion-Weighted MRI. In: Belkić D, Belkić K, editors. Comprehensive Biomedical Physics: Magnetic Resonance Imaging and Spectroscopy. Stockholm: Elsevier B.V; 2014. p. 81–97. https://doi.org/10.1016/b978-0-444-53632-7.00306-3.

[23] Surov A, Meyer HJ, Winter K, Richter C, Hoehn A-K. Histogram analysis parameters of apparent diffusion coefficient reflect tumor cellularity and proliferation activity in head and neck squamous cell carcinoma. Oncotarget 2018;9:23599–607. https://doi.org/10.18632/oncotarget.25284.

[24] Jackson A, Buckley D, Parker GJM. Dynamic contrast-enhanced magnetic resonance imaging in oncology. Berlin: Springer; 2005.

[25] Hui EP, Chan ATC, Pezzella F, Turley H, To K-F, Poon TCW, et al. Coexpression of hypoxia-inducible factors 1alpha and 2alpha, carbonic anhydrase IX, and vascular

endothelial growth factor in nasopharyngeal carcinoma and relationship to survival. Clin Cancer Res 2002;8:2595–604.
[26] Lu X, Wang X, Zhang Y, Hu C, Shen C, Feng Y. Hypoxia Inducible Factor-1α and Vascular Endothelial Growth Factor Expression are Associated with a Poor Prognosis in Patients with Nasopharyngeal Carcinoma Receiving Radiotherapy with Carbogen and Nicotinamide. Clin Oncol 2008;20:606–12. https://doi.org/10.1016/j.clon.2008.07.001.
[27] Arnold F. Tumour angiogenesis. Ann R Coll Surg Engl 1985;67:295–8.
[28] Shukla-Dave A, Obuchowski NA, Chenevert TL, Jambawalikar S, Schwartz LH, Malyarenko D, et al. Quantitative imaging biomarkers alliance (QIBA) recommendations for improved precision of DWI and DCE-MRI derived biomarkers in multicenter oncology trials. J Magn Reson Imaging 2019;49:e101–21. https://doi.org/10.1002/jmri.26518.
[29] Surov A, Meyer HJ, Leifels L, Höhn A-K, Richter C, Winter K. Histogram analysis parameters of dynamic contrast-enhanced magnetic resonance imaging can predict histopathological findings including proliferation potential, cellularity, and nucleic areas in head and neck squamous cell carcinoma. Oncotarget 2018;9:21070–7. https://doi.org/10.18632/oncotarget.24920.